PHYSICAL REVIEW D **80,** 033006 (2009)

Decays $Z \to ggg$ and $Z' \to ggg$ in the minimal 331 model

A. Flores-Tlalpa, J. Montaño, F. Ramírez-Zavaleta, and J. J. Toscano

Facultad de Ciencias Físico Matemáticas, Benemérita Universidad Autónoma de Puebla, Apartado Postal 1152, Puebla, Puebla, México

(Received 9 June 2009; published 24 August 2009)

We perform a complete calculation at the one-loop level for the $Zggg$ and $Z'ggg$ couplings in the context of the minimal 331 model, which predicts the existence of a new Z' gauge boson and new exotic quarks. Bose symmetry is exploited to write a compact and manifest $SU_C(3)$-invariant vertex function for the $Vggg$ ($V = Z, Z'$) coupling. Previous results on the $Z \to ggg$ decay in the standard model are reproduced. It is found that this decay is insensitive to the effects of the new exotic quarks. This in contrast with the $Z' \to ggg$ decay, which is sensitive to both the standard model and exotic quarks, whose branching ratio is larger than that of the $Z \to ggg$ transition by about a factor of 4.

DOI: 10.1103/PhysRevD.80.033006 PACS numbers: 13.38.Dg, 12.60.Cn, 14.70.Dj

I. INTRODUCTION

There are no couplings of gluons with the neutral electroweak gauge bosons ($V = \gamma, Z$) at the level of classical action in a renormalizable theory,[1] but they can be induced via loops. At the one-loop level, only quartic couplings of the type $Vggg$ and $VVgg$ can be generated, as the trilinear Vgg ones are forbidden at any order of perturbation theory by Yang's theorem [2]. In particular, the $Zggg$ coupling is a very interesting prediction of perturbative quantum field theory, which allows one to examine the interplay of the strong interactions and the weak interactions, as it represents a rare case where purely strong interacting particles couple to purely weak interacting particles. Also, this coupling is interesting from the phenomenological point of view, because it is much less suppressed than the purely electroweak couplings $VVVV$. Several authors have studied the decay $Z \to ggg$ in the standard model (SM) [3–6]. The Lorentz structure of this vertex is governed by the vector and axial vector couplings of the Z boson to quarks, which leads to an amplitude made of two finite and gauge-invariant subamplitudes that do not interfere among themselves due to their different color structure. Because of this, both the vector and the axial vector subamplitudes characterizing the $Zggg$ coupling have separately been studied in the literature. It turns out to be that, except for some color factors, the vector part of the $Zggg$ is the same as the four photon interaction in QED [7]. This result was used in Ref. [8] to calculate the $\gamma^* ggg$ coupling, which was further adapted to study the vector $Zggg$ coupling [3]. The contribution of triangle diagrams to the axial vector $Zggg$ coupling was calculated in Ref. [4], which however is not gauge invariant. The complete calculation for the axial vector part, which comprises triangle and box diagrams, was done in Ref. [5]. The impact of the third family is analyzed analytically in the limit $m_b \to 0$ and $m_t \to \infty$ in Ref. [6]. In general terms, as we will see below, both the vector and axial vector amplitudes are essentially determined by the third family, the latter one playing a marginal role with respect to the former.

In this work we are interested in studying the rare decays [9] $Z \to ggg$ and $Z' \to ggg$ within the context of the so-called 331 model [10]. This model, which is based in the $SU_C(3) \times SU_L(3) \times U_X(1)$ gauge group, predicts the existence of new gauge bosons, among them, a new Z' gauge boson that has some interesting features [11], such as the possibility of yielding signals of new physics at the TeV scale. In this model, the lepton spectrum is the same as in the SM, but it is arranged in antitriplets of $SU_L(3)$. The quark sector is also arranged in the fundamental representation of this group, which requires the introduction of three new quarks. An interesting feature of the model is that anomalies cancel out when all of the generations are summed over, which means that the family number must be a multiple of the color number, which suggests a possible approach to solving the generation replication problem. In order to endow all of the particles with mass, a Higgs sector composed by three triplets and one sextet of $SU_L(3)$ is required, though only one of the triplets is needed to break down $SU_L(3) \times U_X(1)$ into $SU_L(2) \times U_Y(1)$ at the new physics scale $u > v$, where $v \approx 246$ GeV is the Fermi scale. In the first stage of spontaneous symmetry breaking (SSB), singly and doubly charged gauge bosons emerge in a doublet of the $SU_L(2)$ group, as well as a new neutral Z' boson. The three exotic quarks (D and S with charge $-4/3$ in units of the positron charge, and T with charge $5/3$) do not couple to the W gauge boson, since they emerge as singlets of $SU_L(2)$ and get their mass at the u scale. However, these exotic quarks do couple to all of the neutral gauge bosons of the theory, namely, Z', Z, γ, and g [12]. Besides studying the impact of the new quarks on the $Z \to ggg$ decay, we are interested

[1]This class of couplings arises at the level of classical action in the noncommutative standard model [1], but this theory is not renormalizable.

in investigating the peculiarities that could present the $Z'ggg$ couplings due to the presence of these exotic quarks, which are singlets under the $SU_L(2)$ group and present both vector and axial vector couplings to Z'. Also, it is interesting to investigate the sensitivity of a new heavy Z' boson to the three standard quark families, as well as to new quark particles. We are motivated by the physics potential of the LHC collider, which will allow one to study directly and in detail the TeV scale region. In particular, the multipurpose ATLAS detector [13] has the mission of detecting or excluding the presence of a new Z' boson in the TeV scale. Therefore, it is important to study the decays of this type of particle, including those rare processes, as the $Z' \to ggg$ transition. We will present exact analytical expressions for the corresponding amplitudes, which will be used to reproduce previous results given in the context of the SM for the $Z \to ggg$ decay.

The paper has been organized as follows. In Sec. II, a brief description of the minimal 331 model is presented with emphasis in the neutral currents sector. In Sec. III, the calculation for the one-loop generated on-shell $Vggg$ vertex is presented. Section IV is devoted to the discussion of our results. In Sec. V, the results are summarized. Finally, some large mathematical expressions are presented in the Appendix.

II. THE MINIMAL 331 MODEL

In this section, we will discuss briefly the main features of the 331 model [10], which is based in the $SU_C(3) \times SU_L(3) \times U_X(1)$ gauge group. As already mentioned in the introduction, the lepton sector of the model is the same as in the SM, but it is now arranged as antitriplets of $SU_L(3)$ as follows:

$$L_i = \begin{pmatrix} l_i \\ \nu_{l_i} \\ l_i^c \end{pmatrix}, (1, 3^*, 0), \qquad i = 1, 2, 3. \tag{1}$$

In order to cancel the $SU_L(3)$ anomaly, the same number of fermion triplets and antitriplets are required. This means that two quark families must be accommodated as triplets and the other one as an antitriplet. It is customary to choose the third family as the one transforming as an antitriplet in order to distinguish the new dynamic effects in the physics of the top quark from that of the lighter families. Accordingly, the three families are specified as follows:

$$\begin{aligned} Q_{1,2} &= \begin{pmatrix} u \\ d \\ D \end{pmatrix}, \begin{pmatrix} c \\ s \\ S \end{pmatrix}, (3, 3, -1/3), \\ Q_3 &= \begin{pmatrix} t \\ b \\ T \end{pmatrix}, (3, 3^*, 2/3), \end{aligned} \tag{2}$$

$$d^c, s^c, b^c: (3^*, 1, 1/3), \qquad D^c, S^c: (3^*, 1, 4/3), \tag{3}$$

$$u^c, c^c, t^c: (3^*, 1, -2/3), \qquad T^c: (3^*, 1, -5/3), \tag{4}$$

where the exotic quarks D, S, and T have electric charges of $-4/3$, $-4/3$, and $5/3$, respectively.

The Higgs sector comprises three triplets and one sextet of $SU_L(3)$, but only one of the triplets is needed to break $SU_L(3) \times U_X(1)$ into $SU_L(2) \times U_Y(1)$. The next stage of SSB occurs at the Fermi scale v and is achieved by the remaining two triplets. The sextet is necessary to provide realistic masses for the leptons [14]. In the first stage of SSB, several particles acquire masses [11,12], among them the new Z' gauge boson and the exotic quarks, which are all singlets of $SU_L(2)$ and thus they do not couple to the W gauge boson at the tree level.[2] Many details of the Z' dynamics have already been presented in Ref. [12]. Very interestingly, in this model the new gauge boson masses are bounded from above [10,12,15] due to the theoretical constraint which yields $\sin^2\theta_W = s_W^2 \leq 1/4$ [10,15]. The fact that the value of s_W^2 is very close to $1/4$ at the $m_{Z'}$ scale leads to an upper bound on the scale associated with the first stage of SSB, which translates directly into a bound on the Z' mass given by $m_{Z'} \leq 3.1$ TeV [15]. It turns out that when $s_W^2(\mu) = 1/4$, the coupling constant g_X associated with the $U_X(1)$ group becomes infinite and a Landau pole arises [16]. Here, we will focus on only those features that are relevant for our discussion. In particular, we need the couplings of the Z and Z' gauges bosons to quarks. The neutral currents of the quark sector of the model can be written as follows [12]:

$$\begin{aligned} \mathcal{L}_q^{\mathrm{NC}} = ie\sum_q Q_q(\bar{q}\gamma_\mu q)A^\mu + \frac{ig}{2c_W}\sum_q [\bar{q}\gamma_\mu(g_{VZ}^q \\ - g_{AZ}^q\gamma_5)qZ^\mu + \bar{q}\gamma_\mu(g_{VZ'}^q - g_{AZ'}^q\gamma_5)qZ'^\mu], \end{aligned} \tag{5}$$

where the electromagnetic current has been included, too. The intensity of the diverse couplings are presented in Table I. In this table, $s_W(c_W)$ stands for $\sin\theta_W(\cos\theta_W)$ of the weak angle. On the other hand, the Feynman rules of QCD are well-known, so we are ready to calculate the amplitude for the on-shell $Vggg$ ($V = Z, Z'$) vertex. This will be carried out in the next section. It should be mentioned that there is a different version of this model [17] which introduces exotic leptons but with the same quark sector. Since both versions the model the quark sector accommodate the same representation of the $SU_L(3) \times U_X(1)$ gauge group, our results are also applicable to this version with exotic leptons.

[2]The $\{Z, Z'\}$ basis does not indeed represent mass eingenstates, but it is related to the mass eigenstates $\{Z_1, Z_2\}$ basis through an orthogonal transformation [12]. The mixing angle is however very small and can be ignored in the present analysis.

TABLE I. Structure of the neutral currents for the quark sector of the minimal 331 model.

Quark	Q_q	g^q_{VZ}	g^q_{AZ}	$g^q_{VZ'}$	$g^q_{AZ'}$
u, c	$+\frac{2}{3}$	$\frac{3-8s_W^2}{6}$	$\frac{1}{2}$	$-\frac{1-6s_W^2}{2\sqrt{3}c_W^2\sqrt{1-4s_W^2}}$	$-\frac{1+2s_W^2}{2\sqrt{3}c_W^2\sqrt{1-4s_W^2}}$
d, s	$-\frac{1}{3}$	$-\frac{3-4s_W^2}{6}$	$-\frac{1}{2}$	$-\frac{1}{2\sqrt{3}c_W^2\sqrt{1-4s_W^2}}$	$-\frac{\sqrt{1-4s_W^2}}{2\sqrt{3}c_W^2}$
D, S	$-\frac{4}{3}$	$\frac{8s_W^2}{3}$	0	$\frac{1-9s_W^2}{\sqrt{3}c_W^2\sqrt{1-4s_W^2}}$	$\frac{1}{\sqrt{3}\sqrt{1-4s_W^2}}$
b	$-\frac{1}{3}$	$-\frac{3-4s_W^2}{6}$	$-\frac{1}{2}$	$\frac{1-2s_W^2}{2\sqrt{3}c_W^2\sqrt{1-4s_W^2}}$	$\frac{1+2s_W^2}{2\sqrt{3}c_W^2\sqrt{1-4s_W^2}}$
t	$+\frac{2}{3}$	$\frac{3-8s_W^2}{6}$	$\frac{1}{2}$	$\frac{1+4s_W^2}{2\sqrt{3}c_W^2\sqrt{1-4s_W^2}}$	$\frac{\sqrt{1-4s_W^2}}{2\sqrt{3}c_W^2}$
T	$+\frac{5}{3}$	$-\frac{10s_W^2}{3}$	0	$-\frac{1-11s_W^2}{\sqrt{3}c_W^2\sqrt{1-4s_W^2}}$	$-\frac{1}{\sqrt{3}\sqrt{1-4s_W^2}}$

III. THE ONE-LOOP $Vggg$ COUPLING

In this section, we present the calculation for the on-shell $Vggg$ ($V = Z, Z'$) vertex. Since the Lorentz structure of the neutral currents is the same for both the Z and Z' gauge bosons, we will present a generic amplitude for the $Vggg$ vertex. We will present explicit expressions for this amplitude in terms of Passarino-Veltman scalar functions [18]. To begin with, we establish our notation and conventions. The momenta, Lorentz indices, and color indices are defined as follows:

$$V_{\mu_4}(p_4) g^a_{\mu_1}(p_1) g^b_{\mu_2}(p_2) g^c_{\mu_3}(p_3), \tag{6}$$

where all momenta are taken incoming. We will present our results in terms of scalar products of the way $p_i \cdot p_j \equiv p_{ij}$, which are adequate to discuss both of the related processes, namely, the $V \to ggg$ decay, which is the purpose of this work, and the $gg \to gV$ reaction, which will be reported in a future communication together with the processes $gg \to \gamma Z$, $gg \to \gamma Z'$, and $gg \to ZZ'$ [19].

We now proceed to describe the calculation. The contribution to the $Vggg$ coupling occurs through box and triangle diagrams, which are shown in Figs. 1 and 2, respectively. There are six box diagrams and six triangle diagrams, but only one is needed to work out one of each class, as the rest are related by Bose symmetry. The invariant amplitude can be written as follows:

$$\mathcal{M}_{Vggg} = \sum_q \mathcal{M}^{\mu_1\mu_2\mu_3\mu_4}_{abc} \epsilon^a_{\mu_1}(p_1, \lambda_1) \epsilon^b_{\mu_2}(p_2, \lambda_2) \times \epsilon^c_{\mu_3}(p_3, \lambda_3) \epsilon_{\mu_4}(p_4, \lambda_4), \tag{7}$$

where the sum is over all quark flavors. This amplitude in turns can be separated into two components as follows:

$$\mathcal{M}^{\mu_1\mu_2\mu_3\mu_4}_{abc} = \mathcal{M}^{\mu_1\mu_2\mu_3\mu_4}_{Babc} + \mathcal{M}^{\mu_1\mu_2\mu_3\mu_4}_{Tabc}, \tag{8}$$

where B and T stand for box and triangle contributions. The Lorentz tensor structure of the amplitude is dictated by color gauge invariance and Bose symmetry. Gauge invariance means that the amplitude must satisfy the following transversality conditions:

$$p_{i\mu_i} \mathcal{M}^{\mu_1\mu_2\mu_3\mu_4}_{abc} = 0, \qquad i = 1, 2, 3, \tag{9}$$

whereas Bose symmetry requires that $\mathcal{M}^{\mu_1\mu_2\mu_3\mu_4}_{abc}$ be symmetric under the interchange of both $i \leftrightarrow j$ ($i, j = 1, 2, 3$) and color indexes. The contribution from the box diagrams displayed in Fig. 1 can be written as

$$\mathcal{M}^{\mu_1\mu_2\mu_3\mu_4}_{Babc} = \sum_{i=1}^{6} \mathcal{F}_i I^{\mu_1\mu_2\mu_3\mu_4}_{Bi}, \tag{10}$$

where

$$\mathcal{F}_{1,4,5} \equiv -g_s^3 g_V N_C \tfrac{1}{4}(d_{abc} + i f_{abc}), \tag{11}$$

$$\mathcal{F}_{2,3,6} \equiv -g_s^3 g_V N_C \tfrac{1}{4}(d_{abc} - i f_{abc}), \tag{12}$$

where d_{abc} and f_{abc} are the totally symmetric and totally antisymmetric structure constants of the color group. The color structure constants can be obtained from the commutation relations $[T^a, T^b] = i f_{abc} T^c$ and the anticommuta-

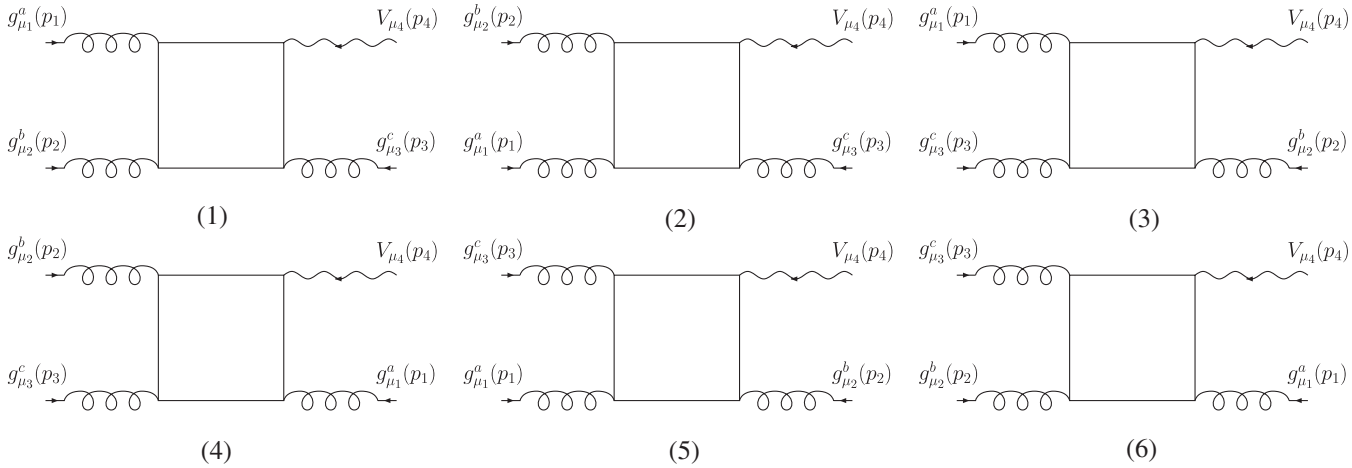

FIG. 1. Box diagrams contributing to the $Vggg$ vertex.

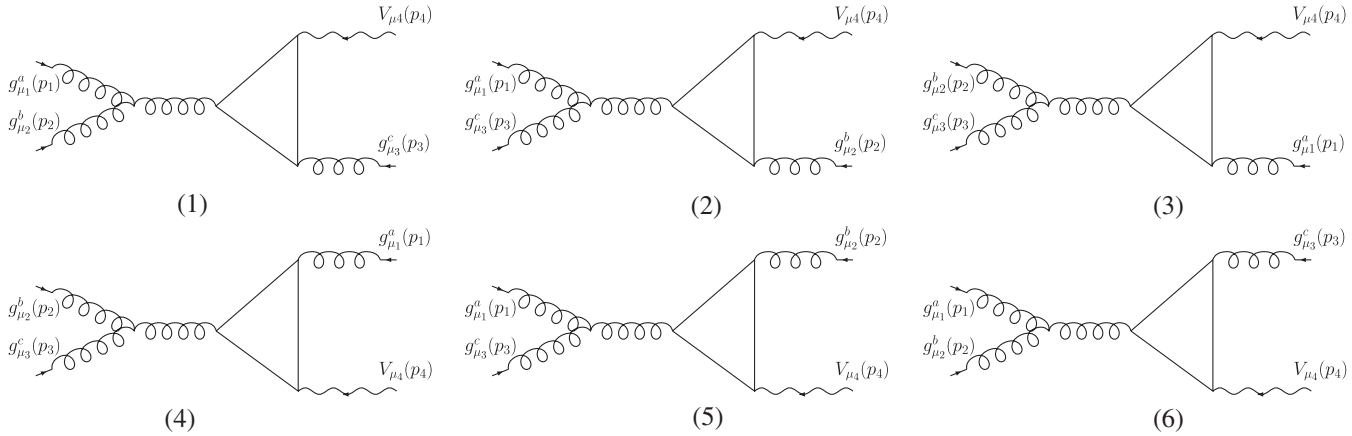

FIG. 2. Triangle diagrams contributing to the $Vggg$ vertex.

tion relations $\{T^a, T^b\} = \delta^{ab}/3 + d_{abc}T^c$ for the $SU_C(3)$ generators. In addition, $g_V = g/2c_W$, and $N_C = 3$ is the quark color number. The $\mathcal{I}_{Bi}^{\mu_1\mu_2\mu_3\mu_4}$ tensors appearing in the above expression are given by

$$\mathcal{I}_{Bi}^{\mu_1\mu_2\mu_3\mu_4} = \int \frac{d^Dk}{(2\pi)^D} \frac{T_{Bi}^{\mu_1\mu_2\mu_3\mu_4}}{\Delta_{Bi}}, \tag{13}$$

where

$$\begin{aligned} T_{B1}^{\mu_1\mu_2\mu_3\mu_4} = \mathrm{Tr}\{&\gamma^{\mu_4}(g_{VV}^q - g_{AV}^q\gamma^5)(\not{k} + m_q) \\ &\times \gamma^{\mu_1}[(\not{k} - \not{p}_1) + m_q] \\ &\times \gamma^{\mu_2}[(\not{k} - \not{p}_1 - \not{p}_2) + m_q] \\ &\times \gamma^{\mu_3}[(\not{k} - \not{p}_1 - \not{p}_2 - \not{p}_3) + m_q]\}, \end{aligned} \tag{14}$$

$$\begin{aligned} \Delta_{B1} = &(k^2 - m_q^2)[(k - p_1)^2 - m_q^2][(k - p_1 - p_2)^2 - m_q^2] \\ &\times [(k - p_1 - p_2 - p_3)^2 - m_q^2]. \end{aligned} \tag{15}$$

The remainding 5 box integrals can be obtained by Bose symmetry as illustrated in Fig. 1.

On the other hand, the contribution arising from the triangle diagrams given in Fig. 2 can be written as follows:

$$\mathcal{M}_{Tabc}^{\mu_1\mu_2\mu_3\mu_4} = \sum_{i=1}^{6} \mathcal{F}'_i \mathcal{I}_{Ti}^{\mu_1\mu_2\mu_3\mu_4}, \tag{16}$$

where

$$\mathcal{F}'_{1,3,4,6} = -g_s^3 g_V N_C\left(-\frac{i}{2} f_{abc}\right), \tag{17}$$

$$\mathcal{F}'_{2,5} = -g_s^3 g_V N_C\left(\frac{i}{2} f_{abc}\right). \tag{18}$$

In the above expression,

$$\mathcal{I}_{Ti}^{\mu_1\mu_2\mu_3\mu_4} = \int \frac{d^Dk}{(2\pi)^D} \frac{T_{Ti}^{\mu_1\mu_2\mu_3\mu_4}}{\Delta_{Ti}}, \tag{19}$$

where

$$\begin{aligned} T_{T1}^{\mu_1\mu_2\mu_3\mu_4} = &\mathrm{Tr}\{\gamma^{\mu_4}(g_{VV}^q - g_{AV}^q\gamma^5)(\not{k} + m_q)\gamma^{\omega}[(\not{k} - \not{p}_1 - \not{p}_2) + m_q]\gamma^{\mu_3}[(\not{k} - \not{p}_1 - \not{p}_2 - \not{p}_3) + m_q]\}\frac{1}{(p_1 + p_2)^2} \\ &\times \left[g_{\omega\rho} + (\xi - 1)\frac{(p_1 + p_2)_\omega (p_1 + p_2)_\rho}{(p_1 + p_2)^2}\right][g^{\mu_2\mu_1}(p_2 - p_1)^\rho + g^{\mu_1\rho}(2p_1 + p_2)^{\mu_2} - g^{\rho\mu_2}(p_1 + 2p_2)^{\mu_1}], \end{aligned} \tag{20}$$

$$\Delta_{T1} = (k^2 - m_q^2)[(k - p_1 - p_2)^2 - m_q^2][(k - p_1 - p_2 - p_3)^2 - m_q^2]. \tag{21}$$

As in the box diagrams case, the remainding 5 triangle integrals can be obtained by Bose symmetry as illustrated in Fig. 2.

Notice that we have introduced the general propagator for the virtual gluon, which depends on the gauge parameter ξ. However, the amplitude is gauge independent, as the longitudinal component of the gluon propagator does not contribute. To solve the above integrals, we have used the Passarino-Veltman tensorial decomposition [18] implemented in the FEYNCALC computer program [20].

Once the loop integrals are solved, the amplitude can be expressed as the sum of the vector part and the axial vector part as follows:

$$\mathcal{M}_{abc}^{\mu_1\mu_2\mu_3\mu_4} = \mathcal{M}_{Vabc}^{\mu_1\mu_2\mu_3\mu_4} + \mathcal{M}_{Aabc}^{\mu_1\mu_2\mu_3\mu_4}. \tag{22}$$

The vector amplitude $\mathcal{M}^{\mu_1\mu_2\mu_3\mu_4}_{Vabc}$ receives contributions only from box diagrams, whereas the axial vector amplitude $\mathcal{M}^{\mu_1\mu_2\mu_3\mu_4}_{Aabc}$ receives contributions from both box diagrams and triangle diagrams. Both amplitudes satisfy separately the transversality conditions

$$p_{i\mu_i}\mathcal{M}^{\mu_1\mu_2\mu_3\mu_4}_{Vabc} = 0, \qquad i = 1, 2, 3, 4, \tag{23}$$

$$p_{i\mu_i}\mathcal{M}^{\mu_1\mu_2\mu_3\mu_4}_{Aabc} = 0, \qquad i = 1, 2, 3. \tag{24}$$

Notice that the vector amplitude also satisfies transversality conditions for the V vector boson. It is important to comment that the axial vector amplitude is transverse only after summing over the box and triangle diagram contributions. Also, each type of diagram leads to a finite amplitude, i.e., the contributions from box and triangle diagrams to the axial vector amplitude are separately finite. Also, Bose symmetry is satisfied separately by each type of diagrams:

$$\begin{aligned}\mathcal{M}^{\mu_1\mu_2\mu_3\mu_4}_{V,AB,ATabc} &= \mathcal{M}^{\mu_1\mu_2\mu_3\mu_4}_{V,AB,ATabc}(p_1, \mu_1, a \leftrightarrow p_2, \mu_2, b) \\ &= \mathcal{M}^{\mu_1\mu_2\mu_3\mu_4}_{V,AB,ATabc}(p_1, \mu_1, a \leftrightarrow p_3, \mu_3, c) \\ &= \mathcal{M}^{\mu_1\mu_2\mu_3\mu_4}_{V,AB,ATabc}(p_2, \mu_2, b \leftrightarrow p_3, \mu_3, c),\end{aligned} \tag{25}$$

where V, AB, AT stand for vector contribution, axial contribution from box diagrams, and axial contribution from triangle diagrams. On the other hand, while the vector amplitude is proportional to d_{abc}, the axial amplitude is proportional to f_{abc}. Accordingly, the vector amplitude can be written as

$$\mathcal{M}^{\mu_1\mu_2\mu_3\mu_4}_{Vabc} = g^q_{VV} d_{abc}\left(-\frac{ig_s^3 g_V N_C}{4\pi^2}\right)\sum_{j=1}^{18} f^q_{V_j} T^{\mu_1\mu_2\mu_3\mu_4}_{V_j}, \tag{26}$$

where the $f^q_{V_j}$ are finite form factors given in terms of Passarino-Veltman scalar functions, which are listed in the Appendix. The $T^{\mu_1\mu_2\mu_3\mu_4}_{V_j}$ Lorentz tensors are gauge structures, i.e., they satisfy

$$p_{j\mu_j} T^{\mu_1\mu_2\mu_3\mu_4}_{V_j} = 0, \qquad j = 1, 2, 3, 4. \tag{27}$$

The set of 18 terms $f^q_{V_j} T^{\mu_1\mu_2\mu_3\mu_4}_{V_j}$ appearing in the vector amplitude can be divided into 3 subsets, each composed of 6 members, all related amongst themselves by Bose symmetry. These subsets can conveniently be organized as follows:

$$\begin{aligned}&\{f^q_{V_1} T^{\mu_1\mu_2\mu_3\mu_4}_{V_1}, \ldots, f^q_{V_6} T^{\mu_1\mu_2\mu_3\mu_4}_{V_6}\}, \\ &\{f^q_{V_7} T^{\mu_1\mu_2\mu_3\mu_4}_{V_7}, \ldots, f^q_{V_{12}} T^{\mu_1\mu_2\mu_3\mu_4}_{V_{12}}\}, \\ &\{f^q_{V_{13}} T^{\mu_1\mu_2\mu_3\mu_4}_{V_{13}}, \ldots, f^q_{V_{18}} T^{\mu_1\mu_2\mu_3\mu_4}_{V_{18}}\}.\end{aligned}$$

In this way, it is only necessary to list one element of each set, for instance, the first one of each subset. Making this choice, the respective gauge structures can be written as

$$\begin{aligned}T^{\mu_1\mu_2\mu_3\mu_4}_{V1} &= (p_1 \cdot p_2 g^{\mu_1\mu_2} - p_2^{\mu_1} p_1^{\mu_2}) \\ &\quad \times (p_1 \cdot p_3 g^{\mu_3\mu_4} - p_1^{\mu_3} p_3^{\mu_4}),\end{aligned} \tag{28}$$

$$\begin{aligned}T^{\mu_1\mu_2\mu_3\mu_4}_{V7} &= (p_1 \cdot p_3 p_2^{\mu_1} - p_1 \cdot p_2 p_3^{\mu_1}) \\ &\quad \times (p_2 \cdot p_3 g^{\mu_2\mu_3} - p_3^{\mu_2} p_2^{\mu_3}) p_2^{\mu_4},\end{aligned} \tag{29}$$

TABLE II. Relations dictated by Bose symmetry among the diverse $d_{abc} f^q_{V_j} T^{\mu_1\mu_2\mu_3\mu_4}_{V_j}$ terms.

$\mathcal{M}^{\mu_1\mu_2\mu_3\mu_4}_{Vabc}$	$p_1, \mu_1, a \leftrightarrow p_2, \mu_2, b$	$p_1, \mu_1, a \leftrightarrow p_3, \mu_3, c$	$p_2, \mu_2, b \leftrightarrow p_3, \mu_3, c$
$d_{abc} f^q_{V1} T_{V1}$	$d_{abc} f^q_{V2} T_{V2}$	$d_{abc} f^q_{V6} T_{V6}$	$d_{abc} f^q_{V3} T_{V3}$
$d_{abc} f^q_{V2} T_{V2}$	$d_{abc} f^q_{V1} T_{V1}$	$d_{abc} f^q_{V5} T_{V5}$	$d_{abc} f^q_{V4} T_{V4}$
$d_{abc} f^q_{V3} T_{V3}$	$d_{abc} f^q_{V5} T_{V5}$	$d_{abc} f^q_{V4} T_{V4}$	$d_{abc} f^q_{V1} T_{V1}$
$d_{abc} f^q_{V4} T_{V4}$	$d_{abc} f^q_{V6} T_{V6}$	$d_{abc} f^q_{V3} T_{V3}$	$d_{abc} f^q_{V2} T_{V2}$
$d_{abc} f^q_{V5} T_{V5}$	$d_{abc} f^q_{V3} T_{V3}$	$d_{abc} f^q_{V2} T_{V2}$	$d_{abc} f^q_{V6} T_{V6}$
$d_{abc} f^q_{V6} T_{V6}$	$d_{abc} f^q_{V4} T_{V4}$	$d_{abc} f^q_{V1} T_{V1}$	$d_{abc} f^q_{V5} T_{V5}$
$d_{abc} f^q_{V7} T_{V7}$	$d_{abc} f^q_{V9} T_{V9}$	$d_{abc} f^q_{V12} T_{V12}$	$d_{abc} f^q_{V8} T_{V8}$
$d_{abc} f^q_{V8} T_{V8}$	$d_{abc} f^q_{V10} T_{V10}$	$d_{abc} f^q_{V11} T_{V11}$	$d_{abc} f^q_{V7} T_{V7}$
$d_{abc} f^q_{V9} T_{V9}$	$d_{abc} f^q_{V7} T_{V7}$	$d_{abc} f^q_{V10} T_{V10}$	$d_{abc} f^q_{V11} T_{V11}$
$d_{abc} f^q_{V10} T_{V10}$	$d_{abc} f^q_{V8} T_{V8}$	$d_{abc} f^q_{V9} T_{V9}$	$d_{abc} f^q_{V12} T_{V12}$
$d_{abc} f^q_{V11} T_{V11}$	$d_{abc} f^q_{V12} T_{V12}$	$d_{abc} f^q_{V8} T_{V8}$	$d_{abc} f^q_{V9} T_{V9}$
$d_{abc} f^q_{V12} T_{V12}$	$d_{abc} f^q_{V11} T_{V11}$	$d_{abc} f^q_{V7} T_{V7}$	$d_{abc} f^q_{V10} T_{V10}$
$d_{abc} f^q_{V13} T_{V13}$	$d_{abc} f^q_{V14} T_{V14}$	$d_{abc} f^q_{V17} T_{V17}$	$d_{abc} f^q_{V16} T_{V16}$
$d_{abc} f^q_{V14} T_{V14}$	$d_{abc} f^q_{V13} T_{V13}$	$d_{abc} f^q_{V18} T_{V18}$	$d_{abc} f^q_{V15} T_{V15}$
$d_{abc} f^q_{V15} T_{V15}$	$d_{abc} f^q_{V17} T_{V17}$	$d_{abc} f^q_{V16} T_{V16}$	$d_{abc} f^q_{V14} T_{V14}$
$d_{abc} f^q_{V16} T_{V16}$	$d_{abc} f^q_{V18} T_{V18}$	$d_{abc} f^q_{V15} T_{V15}$	$d_{abc} f^q_{V13} T_{V13}$
$d_{abc} f^q_{V17} T_{V17}$	$d_{abc} f^q_{V15} T_{V15}$	$d_{abc} f^q_{V13} T_{V13}$	$d_{abc} f^q_{V18} T_{V18}$
$d_{abc} f^q_{V18} T_{V18}$	$d_{abc} f^q_{V16} T_{V16}$	$d_{abc} f^q_{V14} T_{V14}$	$d_{abc} f^q_{V17} T_{V17}$

$$T_{V13}^{\mu_1\mu_2\mu_3\mu_4} = (p_1 \cdot p_3 g^{\mu_1\mu_2} - p_3^{\mu_1} p_1^{\mu_2}) \times (p_2 \cdot p_3 g^{\mu_3\mu_4} - p_2^{\mu_3} p_3^{\mu_4}) + (p_1 \cdot p_2 p_3^{\mu_1} - p_1 \cdot p_3 p_2^{\mu_1}) \times (p_3^{\mu_2} g^{\mu_3\mu_4} - p_3^{\mu_4} g^{\mu_2\mu_3}). \quad (30)$$

The corresponding form factors are listed in the Appendix. The remainding gauge structures and form factors can be easily obtained by Bose symmetry, as indicated in Table II.

We now turn to discuss the mathematical structure of the axial vector amplitude. As already mentioned, this amplitude receives contributions from both box and triangle diagrams, in contrast with the vector amplitude to which only the box diagrams contribute. While the contributions of both box and triangle graphs satisfy separately the Bose symmetry, one needs to sum over both type of contributions in order to obtain invariance under the color group. Because of this, it is more difficult to conciliate both classes of symmetries in order to write a compact expression, as in the vector case. So, while a judicious use of the Schouthen's identity [21] allows us to write the amplitude in terms of 21 Lorentz tensor gauge structures, explicit Bose symmetry is sacrificed. However, we have find that if the number of gauge structures is enhanced to 24, both gauge and Bose symmetries can be maintained in a manifest way. In this basis, the axial vector amplitude can be written as

$$\mathcal{M}_{Aabc}^{\mu_1\mu_2\mu_3\mu_4} = g_{AV}^q f_{abc}\left(-\frac{ig_s^3 g_V N_C}{4\pi^2}\right)\sum_{j=1}^{24} f_{A_j}^q T_{A_j}^{\mu_1\mu_2\mu_3\mu_4}, \quad (31)$$

where the $f_{A_j}^q$ coefficients are Lorentz scalar form factors, whereas the $T_{A_j}^{\mu_1\mu_2\mu_3\mu_4}$ tensors are gauge structures satisfying the transversality conditions

$$p_{j\mu_j} T_{A_j}^{\mu_1\mu_2\mu_3\mu_4} = 0, \qquad j = 1, 2, 3. \quad (32)$$

In this extended basis, the axial vector amplitude can be written in terms of compact expressions. As it occurs for the vector amplitude, in this case the set 24 gauge structures—together with their 24 associated form factors—can be classified into 4 subsets, each composed of 6 elements, all related through Bose symmetry. In this way, it is only necessary to write one representative element of each subset. Accordingly, we have chosen the following representative gauge structures:

$$T_{A1}^{\mu_1\mu_2\mu_3\mu_4} = \epsilon^{\mu_3\mu_4 p_1 p_3}(p_2^{\mu_1} p_1^{\mu_2} - p_1 \cdot p_2 g^{\mu_1\mu_2}), \quad (33)$$

$$T_{A7}^{\mu_1\mu_2\mu_3\mu_4} = (p_3^{\mu_1}\epsilon^{\mu_3\mu_4 p_1 p_3} - p_1 \cdot p_3 \epsilon^{\mu_1\mu_3\mu_4 p_3}) \times (p_1 \cdot p_2 p_3^{\mu_2} - p_2 \cdot p_3 p_1^{\mu_2}), \quad (34)$$

TABLE III. Relations dictated by Bose symmetry among the diverse $f_{abc} f_{A_j}^q T_{A_j}^{\mu_1\mu_2\mu_3\mu_4}$ terms.

$\mathcal{M}_{Aabc}^{\mu_1\mu_2\mu_3\mu_4}$	$p_1, \mu_1, a \leftrightarrow p_2, \mu_2, b$	$p_1, \mu_1, a \leftrightarrow p_3, \mu_3, c$	$p_2, \mu_2, b \leftrightarrow p_3, \mu_3, c$
$f_{abc} f_{A1}^q T_{A1}$	$f_{abc} f_{A2}^q T_{A2}$	$f_{abc} f_{A6}^q T_{A6}$	$f_{abc} f_{A3}^q T_{A3}$
$f_{abc} f_{A2}^q T_{A2}$	$f_{abc} f_{A1}^q T_{A1}$	$f_{abc} f_{A5}^q T_{A5}$	$f_{abc} f_{A4}^q T_{A4}$
$f_{abc} f_{A3}^q T_{A3}$	$f_{abc} f_{A5}^q T_{A5}$	$f_{abc} f_{A4}^q T_{A4}$	$f_{abc} f_{A1}^q T_{A1}$
$f_{abc} f_{A4}^q T_{A4}$	$f_{abc} f_{A6}^q T_{A6}$	$f_{abc} f_{A3}^q T_{A3}$	$f_{abc} f_{A2}^q T_{A2}$
$f_{abc} f_{A5}^q T_{A5}$	$f_{abc} f_{A3}^q T_{A3}$	$f_{abc} f_{A2}^q T_{A2}$	$f_{abc} f_{A6}^q T_{A6}$
$f_{abc} f_{A6}^q T_{A6}$	$f_{abc} f_{A4}^q T_{A4}$	$f_{abc} f_{A1}^q T_{A1}$	$f_{abc} f_{A5}^q T_{A5}$
$f_{abc} f_{A7}^q T_{A7}$	$f_{abc} f_{A8}^q T_{A8}$	$f_{abc} f_{A12}^q T_{A12}$	$f_{abc} f_{A9}^q T_{A9}$
$f_{abc} f_{A8}^q T_{A8}$	$f_{abc} f_{A7}^q T_{A7}$	$f_{abc} f_{A11}^q T_{A11}$	$f_{abc} f_{A10}^q T_{A10}$
$f_{abc} f_{A9}^q T_{A9}$	$f_{abc} f_{A11}^q T_{A11}$	$f_{abc} f_{A10}^q T_{A10}$	$f_{abc} f_{A7}^q T_{A7}$
$f_{abc} f_{A10}^q T_{A10}$	$f_{abc} f_{A12}^q T_{A12}$	$f_{abc} f_{A9}^q T_{A9}$	$f_{abc} f_{A8}^q T_{A8}$
$f_{abc} f_{A11}^q T_{A11}$	$f_{abc} f_{A9}^q T_{A9}$	$f_{abc} f_{A8}^q T_{A8}$	$f_{abc} f_{A12}^q T_{A12}$
$f_{abc} f_{A12}^q T_{A12}$	$f_{abc} f_{A10}^q T_{A10}$	$f_{abc} f_{A7}^q T_{A7}$	$f_{abc} f_{A11}^q T_{A11}$
$f_{abc} f_{A13}^q T_{A13}$	$f_{abc} f_{A14}^q T_{A14}$	$f_{abc} f_{A17}^q T_{A17}$	$f_{abc} f_{A16}^q T_{A16}$
$f_{abc} f_{A14}^q T_{A14}$	$f_{abc} f_{A13}^q T_{A13}$	$f_{abc} f_{A18}^q T_{A18}$	$f_{abc} f_{A15}^q T_{A15}$
$f_{abc} f_{A15}^q T_{A15}$	$f_{abc} f_{A17}^q T_{A17}$	$f_{abc} f_{A16}^q T_{A16}$	$f_{abc} f_{A14}^q T_{A14}$
$f_{abc} f_{A16}^q T_{A16}$	$f_{abc} f_{A18}^q T_{A18}$	$f_{abc} f_{A15}^q T_{A15}$	$f_{abc} f_{A13}^q T_{A13}$
$f_{abc} f_{A17}^q T_{A17}$	$f_{abc} f_{A15}^q T_{A15}$	$f_{abc} f_{A13}^q T_{A13}$	$f_{abc} f_{A18}^q T_{A18}$
$f_{abc} f_{A18}^q T_{A18}$	$f_{abc} f_{A16}^q T_{A16}$	$f_{abc} f_{A14}^q T_{A14}$	$f_{abc} f_{A17}^q T_{A17}$
$f_{abc} f_{A19}^q T_{A19}$	$f_{abc} f_{A21}^q T_{A21}$	$f_{abc} f_{A24}^q T_{A24}$	$f_{abc} f_{A20}^q T_{A20}$
$f_{abc} f_{A20}^q T_{A20}$	$f_{abc} f_{A22}^q T_{A22}$	$f_{abc} f_{A23}^q T_{A23}$	$f_{abc} f_{A19}^q T_{A19}$
$f_{abc} f_{A21}^q T_{A21}$	$f_{abc} f_{A19}^q T_{A19}$	$f_{abc} f_{A22}^q T_{A22}$	$f_{abc} f_{A23}^q T_{A23}$
$f_{abc} f_{A22}^q T_{A22}$	$f_{abc} f_{A20}^q T_{A20}$	$f_{abc} f_{A21}^q T_{A21}$	$f_{abc} f_{A24}^q T_{A24}$
$f_{abc} f_{A23}^q T_{A23}$	$f_{abc} f_{A24}^q T_{A24}$	$f_{abc} f_{A20}^q T_{A20}$	$f_{abc} f_{A21}^q T_{A21}$
$f_{abc} f_{A24}^q T_{A24}$	$f_{abc} f_{A23}^q T_{A23}$	$f_{abc} f_{A19}^q T_{A19}$	$f_{abc} f_{A22}^q T_{A22}$

$$T^{\mu_1\mu_2\mu_3\mu_4}_{A13} = \epsilon^{\mu_1\mu_3\mu_4 p_3}(p_2 \cdot p_3 p_1^{\mu_2} - p_1 \cdot p_2 p_3^{\mu_2}) + \epsilon^{\mu_3\mu_4 p_1 p_3}(p_2^{\mu_1} p_3^{\mu_2} - p_2 \cdot p_3 g^{\mu_1\mu_2}), \quad (35)$$

$$\begin{aligned} T^{\mu_1\mu_2\mu_3\mu_4}_{A19} = {} & p_1 \cdot p_2(p_3^{\mu_2}\epsilon^{\mu_1\mu_3\mu_4 p_2} - p_2^{\mu_3}\epsilon^{\mu_1\mu_2\mu_4 p_3} \\ & - g^{\mu_2\mu_3}\epsilon^{\mu_1\mu_4 p_2 p_3} - p_2 \cdot p_3 \epsilon^{\mu_1\mu_2\mu_3\mu_4}) \\ & + p_2^{\mu_1}(p_2^{\mu_3}\epsilon^{\mu_2\mu_4 p_1 p_3} - p_3^{\mu_2}\epsilon^{\mu_3\mu_4 p_1 p_2} \\ & - g^{\mu_2\mu_3}\epsilon^{\mu_4 p_1 p_2 p_3} - p_2 \cdot p_3 \epsilon^{\mu_2\mu_3\mu_4 p_1}). \end{aligned} \quad (36)$$

The corresponding form factors are listed in the Appendix. Starting from these representative form factors and gauge structures, it is easy to construct explicitly the remainding ones, as it is illustrated in Table III.

IV. RESULTS AND DISCUSSION

In this section, we discuss our results for the branching ratios of the $Z \to ggg$ [9] and $Z' \to ggg$ decays. The expression for the decay width of the $V \to ggg$ transition can be write in a generic way as follows:

$$\begin{aligned} \Gamma(V \to ggg) &= \frac{m_V}{3!256\pi^3}\int_0^1\int_{1-x}^1 |\mathcal{M}|^2 dydx \\ &= \frac{\alpha_s^3(m_V)\alpha N_C^2 m_V}{384\pi^3 c_W^2 s_W^2}\int_0^1\int_{1-x}^1 \\ &\times \sum_{q,q'}\Big[\frac{40}{3}g_{VV}^q g_{VV}^{q'}\Big(\frac{1}{3}\sum_{\lambda_1,\lambda_2,\lambda_3,\lambda_4}\mathcal{V}_q\mathcal{V}_{q'}^*\Big) \\ &+ 24 g_{AV}^q g_{AV}^{q'}\Big(\frac{1}{3}\sum_{\lambda_1,\lambda_2,\lambda_3,\lambda_4}\mathcal{A}_q\mathcal{A}_{q'}^*\Big)\Big]dydx, \end{aligned} \quad (37)$$

where the sums in λ_i represent the boson polarization sums. The last expression was obtained after using the following definition:

$$\begin{aligned} \mathcal{M}_{V\to ggg} &= g_{VV}^q d_{abc}\Big(-\frac{ig_s^3 g_V N_C}{4\pi^2}\Big)\mathcal{V}_q \\ &+ g_{AV}^q f_{abc}\Big(-\frac{ig_s^3 g_V N_C}{4\pi^2}\Big)\mathcal{A}_q, \end{aligned} \quad (38)$$

with

$$\begin{aligned} \mathcal{V}_q &= \sum_{j=1}^{18} f_{V_j}^q T_{V_j}^{\mu_1\mu_2\mu_3\mu_4}\epsilon_{\mu_1}^{*a}(p_1,\lambda_1)\epsilon_{\mu_2}^{*b}(p_2,\lambda_2) \\ &\times \epsilon_{\mu_3}^{*c}(p_3,\lambda_3)\epsilon_{\mu_4}(p_4,\lambda_4), \end{aligned} \quad (39)$$

$$\begin{aligned} \mathcal{A}_q &= \sum_{j=1}^{24} f_{A_j}^q T_{A_j}^{\mu_1\mu_2\mu_3\mu_4}\epsilon_{\mu_1}^{*a}(p_1,\lambda_1)\epsilon_{\mu_2}^{*b}(p_2,\lambda_2) \\ &\times \epsilon_{\mu_3}^{*c}(p_3,\lambda_3)\epsilon_{\mu_4}(p_4,\lambda_4). \end{aligned} \quad (40)$$

The phase space dimensionless variables x and y are defined by

$$x = \frac{2p_1^0}{m_V}, \qquad y = \frac{2p_2^0}{m_V}, \qquad z = \frac{2p_3^0}{m_V}, \quad (41)$$

which satisfy the relation $x + y + z = 2$. In terms of these variables, the scalar products $p_i \cdot p_j$ are given by

$$p_1 \cdot p_2 = \frac{m_V^2}{2}(x + y - 1), \quad (42)$$

$$p_1 \cdot p_3 = \frac{m_V^2}{2}(1 - y), \quad (43)$$

$$p_2 \cdot p_3 = \frac{m_V^2}{2}(1 - x). \quad (44)$$

The definition domain of these variables is $0 \le x \le 1$ and $1 - x \le y \le 1$. Now, we are ready to present numerical results. In obtaining these numerical results, the Passarino-Veltman scalar functions were evaluated numerically using FF-FORTRAN library routines [22].

A. Decay $Z \to ggg$

In the minimal 331 model, the contribution to the decay width of the $Z \to ggg$ transition can be written as the sum of three partial widths:

$$\Gamma(Z \to ggg) = \Gamma_{q_i} + \Gamma_{Q_i} + \Gamma_{q_i - Q_i}, \quad (45)$$

were Γ_{q_i}, Γ_{Q_i}, and $\Gamma_{q_i-Q_i}$ are the contributions of the SM quarks, the exotic quarks, and the interference between these contributions, respectively. Before presenting the numerical values for these quantities, let us present a brief discussion about the decoupling nature of the vector and the axial vector amplitudes when considered as a function of the quark mass. In Fig. 3, the behavior of the vector amplitude ($VVVV$, left panel) and the axial vector amplitude ($AVVV$, right panel) are shown as a function of the quark mass. The behavior is shown for the bare amplitudes $\Gamma(Z \to ggg)/(g_{VZ}^q)^2$ and $\Gamma(Z \to ggg)/(g_{AZ}^q)^2$. It can be seen from this figure that these amplitudes vanish in the heavy mass limit, which shows their decoupling nature. The behavior of the real and imaginary parts of the amplitudes are shown, too. From this figure, it can be appreciated that the width decay reaches its maximum value for a quark mass of about $m_q = 3.2$ GeV and immediately drops to a negligible value. As we will see below, the vector amplitude is dominated by the bottom quark. As it can be appreciated from Fig. 3, the bare axial vector amplitude reaches its maximum value for $m_q = 0.67$ GeV. Since the axial vector couplings of Z to up and down quarks are equal in magnitude but have opposite signs, there is no contribution in the degenerate case, but a maximum contribution is found for the highest mass difference of the members of a family. Consequently, the dominant contribution to this amplitude arises from the third family.

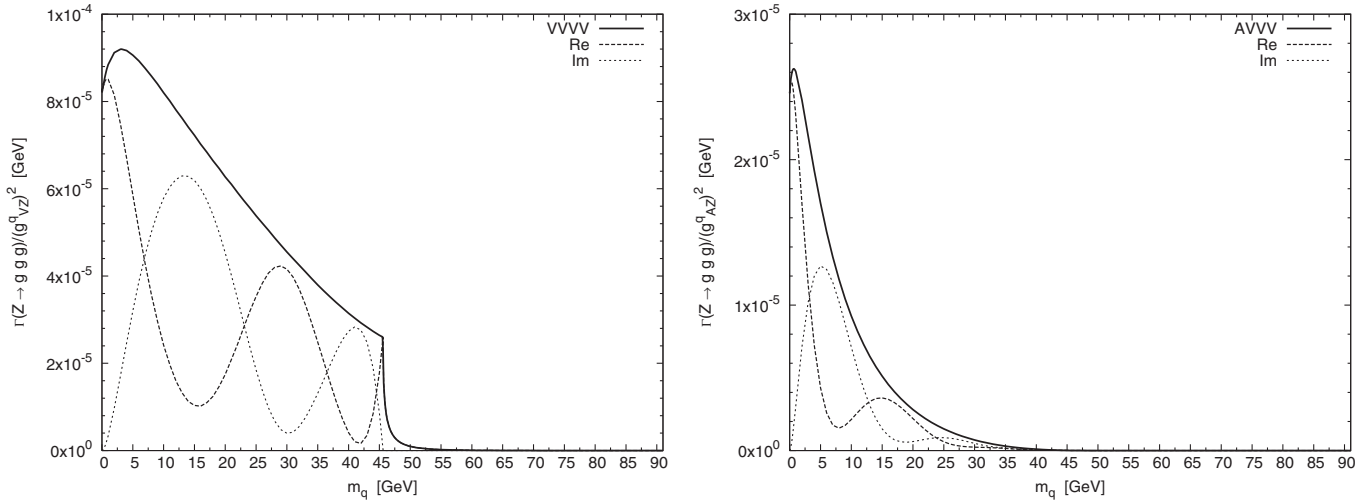

FIG. 3. Decoupling of the vector and the axial vector amplitudes of the $Z \to ggg$ decay when considered as a function of the quark mass. The behavior of both the real and imaginary parts of the amplitudes are shown.

Indeed, both the vector and axial vector amplitudes present a nondecoupling behavior when considered as a function of the mass difference between the members of a family, as they tend to a finite nonzero value for a large mass difference. This behavior, which nicely reproduces the results given in Ref. [6], is shown in Fig. 4.

We now proceed to present numerical results. We will use the following values for the various parameters appearing in the amplitudes [23]: $m_Z = 91.1876$ GeV, $m_u = 0.00255$ GeV, $m_d = 0.00504$ GeV, $m_s = 0.104$ GeV, $m_c = 1.27$ GeV, $m_b = 4.2$ GeV, $m_t = 171.2$ GeV, $s^2_W = 0.23119$, $\alpha_s(m_Z) = 0.1176$, and $\alpha(m_Z) = 1/128$. Regarding the masses of the exotic quarks, the lower bound $m_Q > 240$ GeV was derived from the search for supersymmetry at the Tevatron and would reach the level of 320 at run 2 [24]. In Ref. [25] the production of exotic quarks at THERA and LHC via E_6 theories has been studied, and they have found that exotic quark masses can be high as 450 GeV and 1.2 TeV. It is then reasonable to consider the range $500\ \text{GeV} \leq m_Q \leq 700\ \text{GeV}$ for our numerical analysis. In this scenario we will consider that $m_{D,S,T} = 500$ GeV. With these values, one obtains

$$\Gamma_{q_i} = 3.49 \times 10^{-5}\ \text{GeV}, \tag{46}$$

$$\Gamma_{Q_i} \sim 10^{-12}\ \text{GeV}, \tag{47}$$

$$\Gamma_{q_i - Q_i} \sim 10^{-10}\ \text{GeV}. \tag{48}$$

From these results, it is clear that the exotic quark contribution is absolutely marginal. As far as the contribution of the known quark is concerned, in Table IV more detailed information is presented. From this table, it can be appreciated that both the vector amplitude and the axial vector amplitude are essentially determined by the third family and that the latter is almost 1 order of magnitude lower than the former. All of our results are in perfect agreement with those given in the literature, especially with those presented in Ref. [6].

Finally, the branching ratio for the $Z \to ggg$ decay in the minimal 331 model is given by

$$\text{Br}\,(Z \to ggg) = 1.4 \times 10^{-5}, \tag{49}$$

which is determined essentially by the third family of quarks, as the contribution of the exotic quark is negligible.

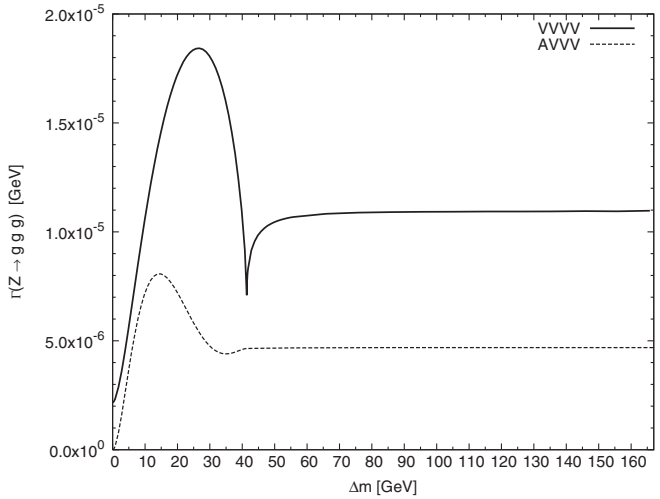

FIG. 4. Nondecoupling of vector and axial vector amplitudes of the $Z \to ggg$ decay as a function of the mass difference of the members of the doublet $\Delta m = m_u - m_d$. The graphic shown corresponds to the case $m_d = 0$.

B. Decay $Z' \to ggg$

We now turn to present numerical results for the $Z' \to ggg$ decay. Although the mathematical structure of the decay width is identical to the one associated with the

TABLE IV. Family contribution to the $\Gamma(Z \to ggg)$ decay in the standard model. Here, Γ^{VI} and Γ^{AI} represent the interference effect induced by the three families into the vector and axial vector width decays, respectively.

Family	Γ^V GeV	Γ^A GeV	Γ^{VI} GeV	Γ^{AI} GeV	Γ_{q_i} GeV	Γ_{Q_i} GeV	$\Gamma_{q_i-Q_i}$ GeV
u, d	1.95×10^{-6}	$\sim 10^{-11}$	...	...	...	...	...
c, s	2.21×10^{-6}	1.5×10^{-6}	...	...	...	...	...
t, b	1.09×10^{-5}	4.69×10^{-6}	...	...	...	...	...
Total	1.51×10^{-5}	6.19×10^{-6}	1.66×10^{-5}	-3.03×10^{-6}	3.49×10^{-5}	$\sim 10^{-12}$	$\sim 10^{-10}$

$Z \to ggg$ decay, its numerical behavior presents some differences due to the fact that the 331 model treats the third family differently compared to the other two. As it can be appreciated from Table I, the main differences between the $Z'\bar{q}q$ and $Z\bar{q}q$ couplings are the following: i) The vector ($g^q_{VZ'}$) and axial vector ($g^q_{AZ'}$) couplings, which are about 1 order of magnitude larger than the respective couplings of the Z boson. As we will see below, these facts lead to partial decay widths larger than those associated with the Z boson. ii) The axial vector couplings of Z' to the members of a doublet are not the negatives of one another, as it occurs for the case of the standard Z boson. iii) The Z' coupling to the third family differs from its couplings to the first two, which are replicas of oneanother. As in the case of the $Z \to ggg$ decay, we express the decay width into three contributions:

$$\Gamma(Z' \to ggg) = \Gamma_{q_i} + \Gamma_{Q_i} + \Gamma_{q_i-Q_i}, \tag{50}$$

where Γ_{q_i}, Γ_{Q_i}, and $\Gamma_{q_i-Q_i}$ are the contributions of the SM quarks, the exotic quarks, and the interference between these contributions, respectively. As far as the Z' boson mass is concerned, although it is not possible to obtain model-independent bounds, current limits from precision experiments imply that $m_{Z'} \gtrsim 500$ GeV [12]. Similar bounds were obtained in Ref. [26] from both the 331 minimal model and the 331 model with right-handed neutrinos. In Ref. [27], a bound for the Z' mass of the order of 300 GeV has been obtained from 331 models at the electroweak scale. Studies in the context of 331 models predict lower bounds greater than 1.5 TeV [28]. In addition, model-dependent upper bounds of the Z' mass are imposed, too, by means of the Landau pole in the context of a perturbative treatment of the model [16], where such bounds are usually estimated around 3 TeV. Therefore, we have considered four scenarios corresponding to $m_{Z'} =$ 500, 1000, 2000, and 3000 GeV for decoupling analysis, to which a maximum value is found for the vector amplitude in values of quark masses of $m_q = 18$, 35, 71, and 107 GeV, respectively. A similar behavior is observed for the axial vector contribution when considered as a function of the quark mass. In Fig. 5, the decoupling nature of the partial vector and axial vector decay widths are shown as a function of the quark mass for the case $m_{Z'} = 1000$ GeV. The nondecoupling nature of both the vector and axial vector contributions, when considered as a function of the mass difference between the members of a doublet, is shown in Figs. 6 and 7. It is interesting to compare these figures with Fig. 4, from which a very different behavior on the nondecoupling nature of the amplitudes can be appreciated.

We now proceed to present numerical results. From now on, we will consider two scenarios, namely, $\{m_{Z'} = m_Q = m_D = m_S = m_T = 500$ GeV$\}$ and $\{m_{Z'} =$ 1500 GeV, $m_Q = m_D = m_S = m_T = 700$ GeV$\}$. The re-

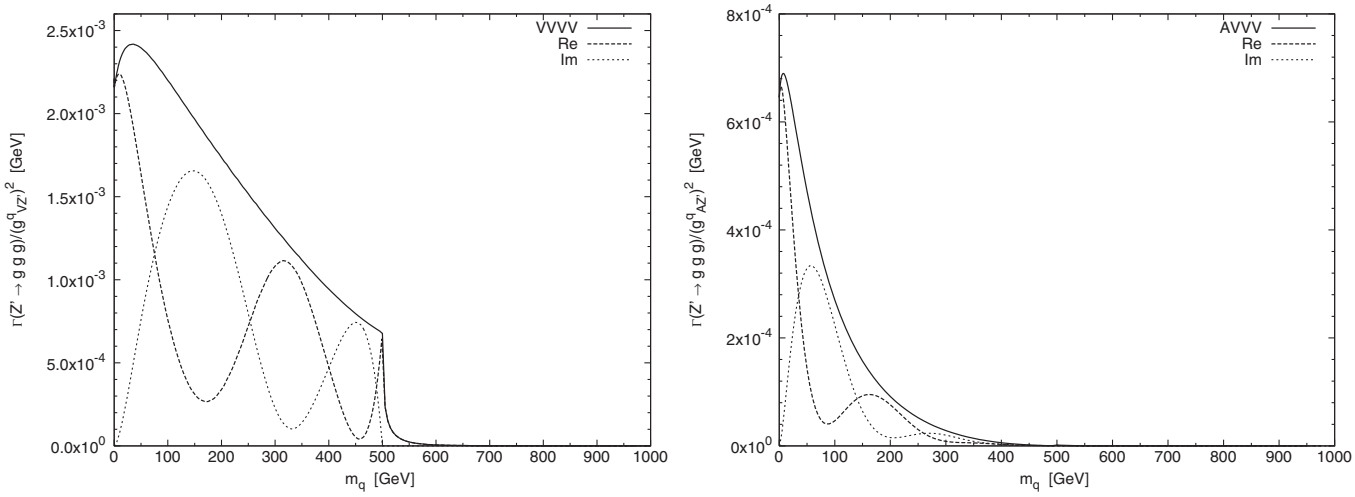

FIG. 5. Decoupling of the vector and the axial vector amplitudes of the $Z' \to ggg$ decay when considered as a function of the quark mass. The behavior of both the real and imaginary parts of the amplitudes are shown.

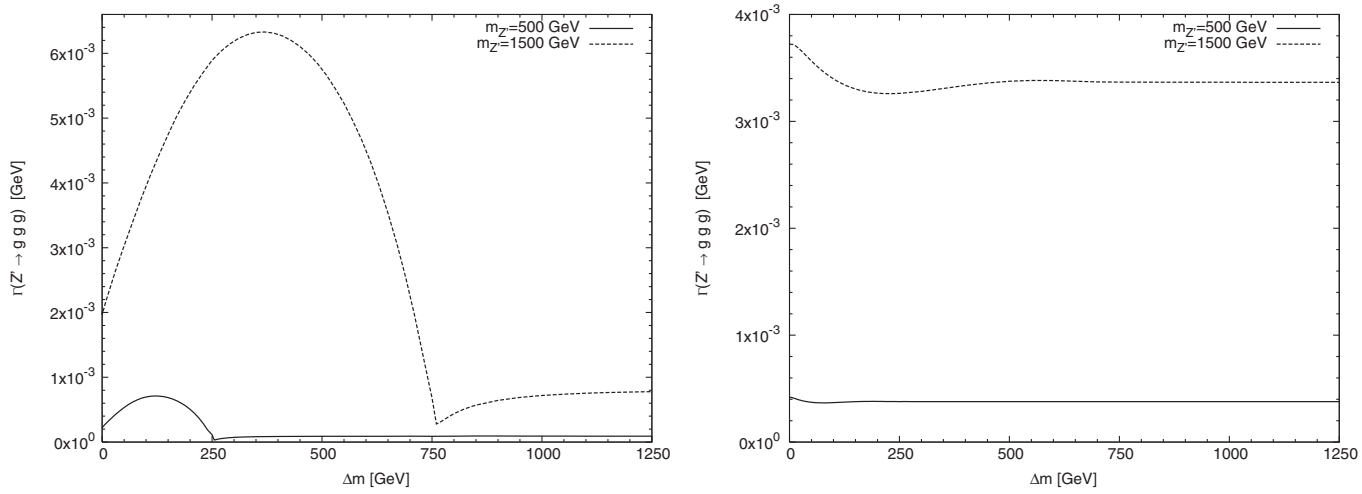

FIG. 6. Nondecoupling behavior of the vector (left) and the axial vector (right) amplitudes of the $Z' \to ggg$ decay when considered as a function of the mass difference of the members of the doublet of the first family. The behavior for the second family is identic.

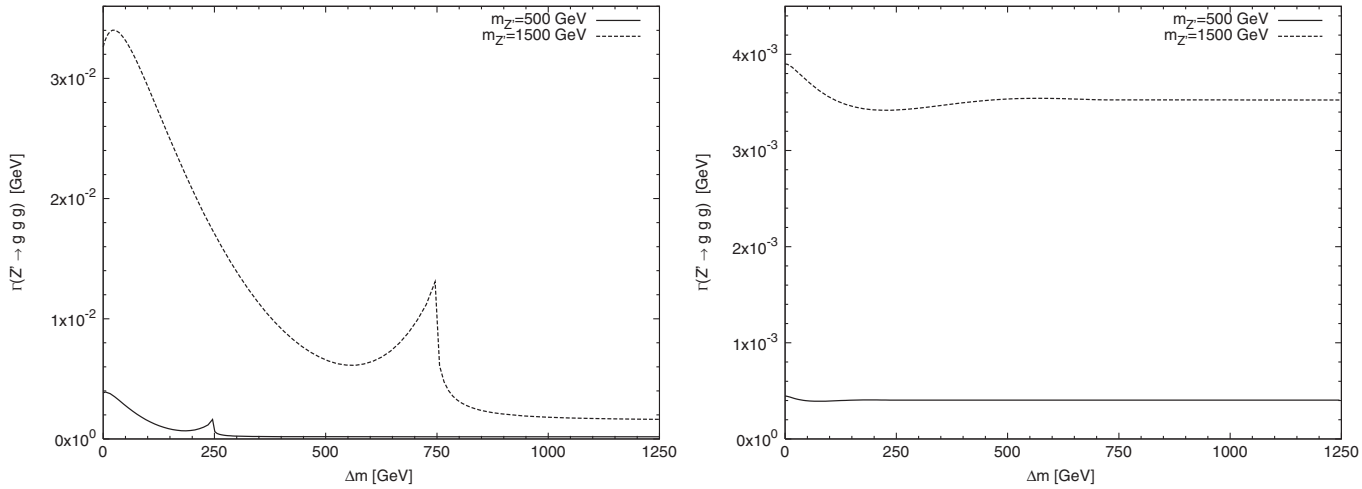

FIG. 7. Nondecoupling behavior of the vector (left) and the axial vector (right) amplitudes of the $Z' \to ggg$ decay when considered as a function of the mass difference of the members of the doublet of the third family.

sults are shown in Table V, where the more important role played by the exotic quarks can be appreciated. Although the contribution of the third family of known quarks to the $Z' \to ggg$ is dominant, as it occurs for the $Z \to ggg$ transition, it should be noticed that in this case there is a significant contribution from the exotic quarks, which tends to be dominant for a heavier Z' boson. This situation is illustrated in Tables VI and VII where the contributions arising from the three families, as well as the interference effects, are shown. In these Tables, we also present the values for α_s obtained from Ref. [23]. On the other hand, the contribution coming from the exotic quarks is shown with some detail in Table VIII, in which the interference effects among exotic quarks is also shown. It is important to notice that the individual contribution of the exotic quarks is so important as those of the known quarks; however, the global contribution is reduced considerably due to an interference effect between the D and S quarks

TABLE V. Partial and total decay widths for the scenarios $\{m_{Z'} = m_Q = m_D = m_S = m_T = 500\ \text{GeV}\}$ and $\{m_{Z'} = 1500\ \text{GeV}, m_Q = m_D = m_S = m_T = 700\ \text{GeV}\}$.

$m_{Z'}$ GeV	m_Q GeV	α_s	Γ_{q_i} GeV	Γ_{Q_i} GeV	$\Gamma_{q_i - Q_i}$ GeV	$\Gamma(Z' \to ggg)$ GeV
500	500	0.104482	2.74×10^{-3}	1.33×10^{-8}	8.97×10^{-6}	2.73×10^{-3}
1500	700	0.150079	2.27×10^{-2}	2.8×10^{-3}	9.11×10^{-3}	3.46×10^{-2}

TABLE VI. Family contribution to the $\Gamma(Z' \to ggg)$ decay in the scenario $m_{Z'} = 500$ GeV. Here, Γ^{VI} and Γ^{AI} represent the interference effect induced by the three families into the vector and axial vector width decays, respectively.

Family	Γ^V GeV	Γ^A GeV	Γ^{VI} GeV	Γ^{AI} GeV	Γ_{q_i} GeV
u, d	2.24×10^{-4}	4.19×10^{-4}	...	...	...
c, s	2.22×10^{-4}	4.36×10^{-4}	...	...	...
t, b	7.18×10^{-4}	4.05×10^{-4}	...	...	...
Total	1.16×10^{-3}	1.26×10^{-3}	1.05×10^{-3}	-7.39×10^{-4}	2.73×10^{-3}

TABLE VII. Family contribution to the $\Gamma(Z' \to ggg)$ decay in the scenario $m_{Z'} = 1500$ GeV. Here, Γ^{VI} and Γ^{AI} represent the interference effect induced by the three families into the vector and axial vector width decays, respectively.

Family	Γ^V GeV	Γ^A GeV	Γ^{VI} GeV	Γ^{AI} GeV	Γ_{q_i} GeV
u, d	2×10^{-3}	3.73×10^{-3}	...	...	...
c, s	1.98×10^{-3}	3.78×10^{-3}	...	...	...
t, b	2.34×10^{-2}	3.44×10^{-3}	...	...	...
Total	2.74×10^{-2}	1.09×10^{-2}	-8.85×10^{-3}	-6.74×10^{-3}	2.27×10^{-2}

TABLE VIII. Exotic quark contribution to the $Z' \to ggg$ decay in the scenario $\{m_{Z'} = 1500$ GeV, $m_Q = m_D = m_S = m_T = 700$ GeV$\}$.

Quark	$\Gamma^V_{Q_i}$ GeV	$\Gamma^V_{Q_{D-S}}$ GeV	$\Gamma^V_{Q_{D-T}}$ GeV	$\Gamma^V_{Q_{S-T}}$ GeV	$\Gamma^A_{Q_i}$ GeV	$\Gamma^A_{Q_{D-S}}$ GeV	$\Gamma^A_{Q_{D-T}}$ GeV	$\Gamma^A_{Q_{S-T}}$ GeV
D	8.58×10^{-3}	...	-...	...	6.05×10^{-6}	...	...	...
S	8.58×10^{-3}	...	...	...	6.05×10^{-6}	...	...	...
T	1.76×10^{-2}	...	...	...	6.05×10^{-6}	...	...	...
D, S	...	1.71×10^{-2}	...	...	...	1.21×10^{-5}	...	...
D, T	...	...	-2.45×10^{-2}	...	...	...	-1.21×10^{-5}	...
S, T	...	...	...	-2.45×10^{-2}	...	...	...	-1.21×10^{-5}

with the T quark, which is a direct consequence of the way in which they appear in the $SU_L(3)$ fundamental representation.

Using the results given in Ref. [12] for the total decay width of the Z' boson, the corresponding branching ratio is given by

$$\mathrm{Br}(Z' \to ggg) = 2.15 \times 10^{-5} \tag{51}$$

for the scenario characterized by a mass of $m_{Z'} = 500$ GeV and

$$\mathrm{Br}(Z' \to ggg) = 4.95 \times 10^{-5} \tag{52}$$

for the scenario with $m_{Z'} = 1500$ GeV.

V. SUMMARY

In this paper, a comprehensive analysis of the rare $Z \to ggg$ and $Z' \to ggg$ decays in the context of the minimal 331 model has been presented. Explicit expressions for the amplitudes generated at the one-loop level given in terms of Passarino-Veltman scalar functions are presented. The fact that the $Vggg$ vertex ($V = Z, Z'$) is governed by the Bose symmetry is exploited to write its associated vertex function in a compact and manifest $SU_C(3)$-invariant way. The total amplitude is composed by the vector amplitude and the axial vector amplitude, which are finite and gauge invariant by themselves and do not interfere among themselves, as they are proportional to the color structures d_{abc} and f_{abc}, respectively. While the axial vector amplitude receives contributions from both box and triangle diagrams and can be expressed in terms of 24 form factors, the vector amplitude arises only from box diagrams and comprises 18 form factors. It turns out to be that each type of diagram (box or triangle) leads to amplitudes which are free of ultraviolet divergences and satisfy Bose symmetry. However, in the case of the axial vector amplitude, gauge invariance is obtained only after summing over the contributions arising from box and triangle diagrams. It is found that the vector amplitude also satisfies the transversality conditions with respect to the V vector boson, which means that in this amplitude, this vector boson appears only through the $V_{\mu\nu} = \partial_\mu V_\nu - \partial_\nu V_\mu$ tensor field. This property is not present in the axial vector amplitude, which is transverse only with respect to the gluonic fields. Our results are valid for any renormalizable theory and are model independent in this sense.

As far as the numerical results are concerned, the behavior of the vector and axial vector amplitudes are analyzed as a function of the mass quark and also as a function of the mass difference of the members of the quark family.

It was found that both types of amplitudes show a decoupling nature with respect to the former case, whereas a nondecoupling behavior is shown with respect to the latter case. In the case of the $Z \to ggg$ decay, the axial vector amplitude vanishes in the degenerate case and reaches its maximum value for the third family. The axial vector contribution to this decay is marginal, as it is almost 1 order of magnitude lower than that associated to the vector amplitude. This decay is insensitive to the presence of exotic quarks, as it is essentially governed by the third family, especially by the bottom quark, whose branching ratio is given by $\mathrm{Br}(Z \to ggg) = 1.4 \times 10^{-5}$. All results given in the literature were nicely reproduced. As for the $Z' \to ggg$ decay, its behavior presents some differences with respect to the standard $Z \to ggg$ decay, as it couples differently to the SM quarks. In particular, its couplings to the third family of quarks differs from its couplings to the first and second families, as in the 331 model in which the former is accommodated as an antitriplet of $SU_L(3)$, whereas the latter two are introduced as triplets of this group. In this case, the axial vector amplitude does not vanish in the degenerate case and its contribution is, in some scenarios, as important as the one given by the vector amplitude. In a scenario with $m_{Z'} = 500$ GeV, the three families give contributions of the same order of magnitude to both the vector amplitude and the axial vector amplitude. The situation changes substantially for a heavier Z' boson, as the vector amplitude receives a dominant contribution from the third family, especially from the top quark. In this case, the contribution of the exotic quarks is much less marginal than in the case of the $Z \to ggg$ decay, and tends to assume a dominant role for a heavier Z' boson. Although the separate contribution of each exotic quark is as important as the one arising from the known quarks, there is an interference effect between the D and S quarks with the T quark that reduces their global contribution by about 1 order of magnitude. For instance, in a scenario with $m_{Z'} = 1500$ GeV, this contribution is 1 order of magnitude lower than that arising from the known quarks, but it tends to increase with the Z' mass. In this scenario, the contribution of the third family to the vector amplitude is 1 order of magnitude larger than the corresponding contribution of the other two families and also 1 order of magnitude larger than the axial vector component of the decay width, which receives contributions of the same order of magnitude from the three families. Thus, while the $Z \to ggg$ decay is governed by the third family, the $Z' \to ggg$ one receives important contributions from the three families. The contribution of exotic quarks to the $Z \to ggg$ decay is completely marginal, but they play a significant role in the case of the $Z' \to ggg$ decay, especially for a relatively heavy Z' boson. In general terms, the decay width for $Z' \to ggg$ is almost 3 orders of magnitude larger than that for $Z \to ggg$. Also, the $Z' \to ggg$ decay has a branching ratio larger than the $Z \to ggg$ decay, which is of $Br(Z' \to ggg) = 2.15 \times 10^{-5}$ and $\mathrm{Br}(Z' \to ggg) = 4.95 \times 10^{-5}$ for $m_{Z'} = 500$ GeV and $m_{Z'} = 1500$ GeV, respectively.

ACKNOWLEDGMENTS

We acknowledge financial support from CONACYT and SNI (México).

APPENDIX: FORM FACTORS OF THE *Vggg* VERTEX

The 3 representative vector form factors are given by

$$
\begin{aligned}
f^q_{V1} = &-\frac{B_0(1)(p_{13}-2p_{23})}{6p_{13}^2p_{23}} + \frac{B_0(3)(2p_{12}-p_{13})p_{23}}{6p_{12}^2p_{13}^2} - \frac{B_0(2)(p_{12}+p_{23})}{6p_{12}^2p_{23}} - \frac{C_0(2)p_{13}(2p_{12}^3+3p_{23}^2p_{12}+2p_{23}^3)}{12p_{12}^3p_{23}^2} \\
&+ \frac{B_0(4)(p_{12}+p_{13}+p_{23})[p_{12}(p_{13}-2p_{23})+p_{13}p_{23}]}{6p_{12}^2p_{13}^2p_{23}} + \frac{D_0(1)[2p_{23}^2m_q^4+p_{12}(2p_{13}-3p_{23})p_{23}m_q^2+2p_{12}^2p_{13}^2]}{6p_{12}p_{13}p_{23}^2} \\
&+ \frac{C_0(4)(p_{13}+p_{23})(2p_{13}^3-3p_{23}^2p_{13}-4p_{23}^3)}{12p_{13}^3p_{23}^2} + \frac{C_0(5)(p_{12}+p_{23})[2p_{13}p_{12}^3+3(2m_q^2+p_{13})p_{23}^2p_{12}+2p_{13}p_{23}^3]}{12p_{12}^3p_{13}p_{23}^2} \\
&- \frac{C_0(6)(p_{12}+p_{13})[(3p_{13}+4p_{23})p_{12}^3-3p_{13}^3p_{12}-2p_{13}^3p_{23}]}{12p_{12}^3p_{13}^3} + C_0(1)\left[\frac{1}{12}p_{12}\left(\frac{3p_{13}+4p_{23}}{p_{13}^3}-\frac{2}{p_{23}^2}\right)-\frac{m_q^2}{2p_{12}p_{13}}\right] \\
&+ \frac{C_0(3)p_{23}[(3p_{13}+4p_{23})p_{12}^3-3p_{13}^2(2m_q^2+p_{13})p_{12}-2p_{13}^3p_{23}]}{12p_{12}^3p_{13}^3} - \frac{1}{6p_{12}p_{13}} \\
&+ \frac{D_0(3)[2p_{12}^2m_q^4+p_{12}(-3p_{12}^2+3p_{13}p_{12}+5p_{13}p_{23})m_q^2+p_{13}^2p_{23}(3p_{12}+2p_{23})]}{6p_{12}^3p_{13}} \\
&+ \frac{D_0(2)\{2p_{13}^2m_q^4+p_{13}[3p_{13}(p_{13}+p_{23})-p_{12}(3p_{13}+4p_{23})]m_q^2-p_{12}^2p_{23}(3p_{13}+4p_{23})\}}{6p_{12}p_{13}^3},
\end{aligned}
\tag{A1}
$$

$$
\begin{aligned}
f_{V7}^{q} = {} & \frac{D_0(2)m_q^2}{2p_{23}^2}\left(\frac{2m_q^2}{p_{12}} + \frac{p_{23}}{p_{13}}\right) + \frac{D_0(3)[2p_{12}m_q^2 + (p_{12} + 2p_{13})p_{23}]m_q^2}{2p_{12}^2p_{23}^2} - \frac{C_0(3)m_q^2}{2p_{12}^2p_{23}} + \frac{C_0(6)(p_{12} + p_{13})^2m_q^2}{2p_{12}^2p_{13}p_{23}^2} \\
& + \frac{B_0(4)(p_{12} + p_{13} + p_{23})(2p_{12} + 3p_{23})}{2p_{23}^3(p_{12} + p_{23})^2} - \frac{C_0(1)(2p_{13} + p_{23})(p_{23}m_q^2 + p_{12}p_{13})}{2p_{13}p_{23}^4} + \frac{1}{2p_{23}^2(p_{12} + p_{23})} - \frac{B_0(1)}{p_{23}^3} \\
& + \frac{C_0(4)(p_{13} + p_{23})[2p_{23}m_q^2 + p_{12}(2p_{13} + p_{23})]}{2p_{12}p_{23}^4} - \frac{B_0(2)[p_{12}(2p_{13} + p_{23}) + p_{23}(3p_{13} + p_{23})]}{2p_{23}^3(p_{12} + p_{23})^2} \\
& + \frac{C_0(5)[(2p_{13} + p_{23})p_{12}^4 + 2p_{23}(m_q^2 + 2p_{13} + p_{23})p_{12}^3 + p_{23}^2(3m_q^2 + 2p_{13} + p_{23})p_{12}^2 + m_q^2p_{23}^4]}{2p_{12}^2p_{23}^4(p_{12} + p_{23})} \\
& + \frac{D_0(1)[2p_{23}^2m_q^4 + p_{12}p_{23}(8p_{13} + 3p_{23})m_q^2 + 2p_{12}^2p_{13}(2p_{13} + p_{23})]}{2p_{12}p_{23}^4} \\
& - \frac{C_0(2)[p_{13}p_{23}^2m_q^2 + p_{12}p_{23}(2p_{13} + p_{23})m_q^2 + p_{12}^2p_{13}(2p_{13} + p_{23})]}{2p_{12}^2p_{23}^4},
\end{aligned} \tag{A2}
$$

$$
\begin{aligned}
f_{V13}^{q} = {} & \frac{B_0(3)(4p_{12} + p_{13})}{12p_{12}p_{13}^2} - \frac{C_0(6)(p_{12} + p_{13})(4p_{12}^3 + p_{13}^3)}{12p_{12}^2p_{13}^3} + \frac{B_0(2)(p_{23} - 8p_{12})}{12p_{12}p_{23}^2} + C_0(3)\left(\frac{p_{23}}{12p_{12}^2} + \frac{p_{12}p_{23}}{3p_{13}^3}\right) \\
& + \frac{D_0(2)(p_{13}^2m_q^4 - 2p_{12}p_{13}p_{23}m_q^2 - 2p_{12}^2p_{23}^2)}{3p_{13}^3p_{23}} + \frac{D_0(3)[2p_{12}^2m_q^4 + p_{12}(3p_{12} - p_{13})p_{23}m_q^2 - p_{13}^2p_{23}^2]}{6p_{12}^2p_{13}p_{23}} \\
& - \frac{C_0(1)p_{12}[8p_{12}p_{13}^3 + 3(2m_q^2 + p_{13})p_{23}p_{13}^2 - 4p_{12}p_{23}^3]}{12p_{13}^3p_{23}^3} + \frac{2p_{13} - p_{23}}{6p_{23}p_{13}^2 + 6p_{23}^2p_{13}} \\
& + \frac{C_0(2)[-8p_{13}p_{12}^3 - 3(2m_q^2 + p_{13})p_{23}p_{12}^2 + p_{13}p_{23}^3]}{12p_{12}^2p_{23}^3} \\
& + \frac{C_0(5)(p_{12} + p_{23})[8p_{13}p_{12}^3 + 3(2m_q^2 + p_{13})p_{23}p_{12}^2 - p_{13}p_{23}^3]}{12p_{12}^2p_{13}p_{23}^3} \\
& + \frac{B_0(1)[-8p_{12}p_{13}^3 - 3(4p_{12} + p_{13})p_{23}p_{13}^2 + 6p_{12}p_{23}^2p_{13} + (4p_{12} + 3p_{13})p_{23}^3]}{12p_{13}^2p_{23}^2(p_{13} + p_{23})^2} \\
& + \frac{B_0(4)(p_{12} + p_{13} + p_{23})[2p_{12}(4p_{13}^3 + 6p_{23}p_{13}^2 - 3p_{23}^2p_{13} - 2p_{23}^3) - p_{13}p_{23}(p_{13} + p_{23})^2]}{12p_{12}p_{13}^2p_{23}^2(p_{13} + p_{23})^2} \\
& + \frac{D_0(1)\{8p_{12}^2p_{13}^2 + p_{12}(14m_q^2 + 3p_{13})p_{23}p_{13} + m_q^2p_{23}^2[2m_q^2 + 3(p_{13} + p_{23})]\}}{6p_{13}p_{23}^3} \\
& + \frac{C_0(4)\{3p_{23}[2(p_{13}^2 + 2p_{23}p_{13} - p_{23}^2)m_q^2 + p_{13}(p_{13} + p_{23})^2]p_{13}^2 + 4p_{12}(p_{13} + p_{23})^2(2p_{13}^3 - p_{23}^3)\}}{12p_{13}^3p_{23}^3(p_{13} + p_{23})}.
\end{aligned} \tag{A3}
$$

The 4 representative axial vector form factors are given by

$$
\begin{aligned}
f_{A1}^{q} = {} & \frac{1}{4p_{12}^3}\Bigg\{-\frac{2p_{12}^2}{p_{12} + p_{13}} + 2p_{12}[B_0(2) - B_0(4)] + \frac{2p_{12}[p_{13}p_{23} + p_{12}(p_{12} + p_{13} + 2p_{23})][B_0(3) - B_0(4)]}{(p_{12} + p_{13})^2} \\
& + (p_{12} + 2p_{23})[p_{13}C_0(2) + p_{23}C_0(3)] - \frac{(p_{12} + p_{23})[2m_q^2p_{12} + p_{13}(p_{12} + 2p_{23})]C_0(5)}{p_{13}} \\
& + \frac{2m_q^2p_{12}(p_{13} + p_{23})C_0(4)}{p_{13}} - \frac{[2m_q^2p_{12}(p_{13}^2 + 2p_{12}p_{13} - p_{12}^2) + p_{13}(p_{12} + p_{13})^2(p_{12} + 2p_{23})]C_0(6)}{p_{13}(p_{12} + p_{13})} \\
& + \frac{2m_q^2p_{12}^2(p_{13} + p_{23})D_0(2)}{p_{13}} - 2[m_q^2p_{12}(p_{12} + 3p_{23}) + p_{13}p_{23}(p_{12} + 2p_{23})]D_0(3)\Bigg\},
\end{aligned} \tag{A4}
$$

$$f^q_{A7} = \frac{1}{2p_{12}p_{13}^3}\Big\{\frac{p_{13}^2(p_{13}^2 - p_{12}p_{23})}{p_{23}(p_{12}+p_{13})(p_{13}+p_{23})} + \frac{p_{12}p_{13}(2p_{13}+p_{23})[B_0(1)-B_0(4)]}{(p_{13}+p_{23})^2} + \frac{p_{12}p_{13}(p_{12}+2p_{13})[B_0(3)-B_0(4)]}{(p_{12}+p_{13})^2}$$
$$+ p_{12}^2 C_0(1) + p_{12}p_{23}C_0(3) - \frac{[m_q^2 p_{13}(p_{23}^2 + 2p_{13}p_{23} - p_{13}^2) + p_{12}p_{23}(p_{13}+p_{23})^2]C_0(4)}{p_{23}(p_{13}+p_{23})}$$
$$+ \frac{m_q^2 p_{13}(p_{12}+p_{23})C_0(5)}{p_{23}} - \frac{[m_q^2 p_{13}(p_{12}^2 + 2p_{12}p_{13} - p_{13}^2) + p_{12}p_{23}(p_{12}+p_{13})^2]C_0(6)}{p_{23}(p_{12}+p_{13})} + \frac{m_q^2 p_{12}p_{13}^2 D_0(1)}{p_{23}}$$
$$- p_{12}(3m_q^2 p_{13} + 2p_{12}p_{23})D_0(2) + m_q^2 p_{13}^2 D_0(3)\Big\}, \tag{A5}$$

$$f^q_{A13} = \frac{1}{4}\Big\{\frac{2[p_{13}p_{23} + p_{12}(p_{13}+2p_{23})]}{p_{12}p_{23}(p_{12}+p_{13})(p_{13}+p_{23})} + \frac{(p_{13}^2 - 2p_{13}p_{23} - p_{23}^2)[B_0(1)-B_0(4)]}{p_{13}p_{23}(p_{13}+p_{23})^2} - \frac{B_0(2)-B_0(4)}{p_{12}p_{23}}$$
$$- \frac{(p_{12}^2 + 4p_{12}p_{13} + p_{13}^2)[B_0(3)-B_0(4)]}{p_{12}p_{13}(p_{12}+p_{13})^2} - \frac{p_{12}C_0(1)}{p_{13}^2} - \frac{p_{13}C_0(2)}{p_{12}^2} - \frac{p_{23}(p_{12}^2+p_{13}^2)C_0(3)}{p_{12}^2 p_{13}^2}$$
$$+ \frac{[4m_q^2 p_{13}^2 + p_{12}(p_{13}+p_{23})^2]C_0(4)}{p_{12}p_{13}^2(p_{13}+p_{23})} + \frac{(p_{12}+p_{23})C_0(5)}{p_{12}^2} + \frac{[4m_q^2 p_{12}^2 p_{13}^2 + p_{23}(p_{12}+p_{13})^2(p_{12}^2+p_{13}^2)]C_0(6)}{p_{23}p_{12}^2 p_{13}^2(p_{12}+p_{13})}$$
$$+ \frac{2[m_q^2 p_{13}(p_{13}+p_{23}) + p_{12}p_{23}^2]D_0(2)}{p_{23}p_{13}^2} - \frac{2[m_q^2 p_{12}(p_{12}-p_{23}) - p_{13}p_{23}^2]D_0(3)}{p_{23}p_{12}^2}\Big\}, \tag{A6}$$

$$f^q_{A19} = \frac{1}{4}\Big\{-\frac{2}{p_{23}(p_{12}+p_{13})} + \frac{2[B_0(2)-B_0(4)]}{p_{12}(p_{12}+p_{23})} + \frac{2[B_0(3)-B_0(4)]}{(p_{12}+p_{13})^2} + \frac{p_{13}C_0(2)}{p_{12}^2} + \frac{p_{23}C_0(3)}{p_{12}^2} - \frac{(p_{12}+p_{23})C_0(5)}{p_{12}^2}$$
$$- \frac{[4m_q^2 p_{12}^2 + p_{23}(p_{12}+p_{13})^2]C_0(6)}{p_{23}p_{12}^2(p_{12}+p_{13})} + \frac{2m_q^2[D_0(1)-D_0(2)]}{p_{12}} - \frac{2(m_q^2 p_{12} + p_{13}p_{23})D_0(3)}{p_{12}^2}\Big\}. \tag{A7}$$

In writing the above expressions we have introduced the following definitions:

$B_0(1) \equiv B_0(2p_{12}, m_q^2, m_q^2)$, $B_0(2) \equiv B_0(2p_{13}, m_q^2, m_q^2)$, $B_0(3) \equiv B_0(2p_{23}, m_q^2, m_q^2)$,
$B_0(4) \equiv B_0(m_V^2, m_q^2, m_q^2)$, $C_0(1) \equiv C_0(0, 0, 2p_{12}, m_q^2, m_q^2, m_q^2)$, $C_0(2) \equiv C_0(0, 0, 2p_{13}, m_q^2, m_q^2, m_q^2)$,
$C_0(3) \equiv C_0(0, 0, 2p_{23}, m_q^2, m_q^2, m_q^2)$, $C_0(4) \equiv C_0(0, 2p_{12}, m_V^2, m_q^2, m_q^2, m_q^2)$, $C_0(5) \equiv C_0(0, 2p_{13}, m_V^2, m_q^2, m_q^2, m_q^2)$,
$C_0(6) \equiv C_0(0, 2p_{23}, m_V^2, m_q^2, m_q^2, m_q^2)$, $D_0(1) \equiv D_0(0, 0, 0, m_V^2, 2p_{12}, 2p_{13}, m_q^2, m_q^2, m_q^2, m_q^2)$,
$D_0(2) \equiv D_0(0, 0, 0, m_V^2, 2p_{12}, 2p_{23}, m_q^2, m_q^2, m_q^2, m_q^2)$, $D_0(3) \equiv D_0(0, 0, 0, m_V^2, 2p_{13}, 2p_{23}, m_q^2, m_q^2, m_q^2, m_q^2)$,

where $p_{ij} \equiv p_i \cdot p_j$, with $i, j = 1, 2, 3$.

[1] X. Calmet, B. Jurco, P. Schupp, J. Wess, and M. Wohlgenannt, Eur. Phys. J. C **23**, 363 (2002).
[2] C. N. Yang, Phys. Rev. **77**, 242 (1950); L. D. Landau, Dokl. Akad. Nauk, SSSR **60**, 207 (1948).
[3] M. L. Laursen, K. O. Mikaelian, and M. A. Samuel, Phys. Rev. D **23**, 2795 (1981); **25**, 710 (1982); M. L. Laursen and M. A. Samuel, Z. Phys. C **14**, 325 (1982); M. L. Laursen, M. A. Samuel, G. B. Tupper, and A. Sen, Phys. Rev. D **27**, 196 (1983).
[4] S. C. Lee and W. C. Su, Phys. Rev. D **38**, 414 (1988).
[5] J. J. van der Bij and E. W. N. Glover, Nucl. Phys. **B313**, 237 (1989).
[6] R. Hopker and J. J. van der Bij, Phys. Rev. D **49**, 3779 (1994).
[7] V. Costantini, B. De Tollis, and G. Pistoni, Nuovo Cimento Soc. Ital. Fis. **2A**, 733 (1971).
[8] V. N. Baier, E. A. Kurayev, and V. S. Fadin, Yad. Fiz. **31**, 700 (1980) [Sov. J. Nucl. Phys. **31**, 364 (1980)].
[9] For some reviews on rare Z decays, see E. W. N. Glover and J. J. van der Bij, in *Z. Physics at LEP-1, Proceedings of the Workshop, Geneva, Switzerland, September 4-5, 1989*, edited by G. Altarelli *et al.* (CERN Yellow Report No. 89-90, 1989); M. A. Pérez, G. Tavares-Velasco, and J. J. Toscano, Int. J. Mod. Phys. A **19**, 159 (2004).

[10] F. Pisano and V. Pleitez, Phys. Rev. D **46**, 410 (1992); P. H. Frampton, Phys. Rev. Lett. **69**, 2889 (1992).
[11] Some features of the 331 model are discussed in G. Tavares-Velasco and J. J. Toscano, Phys. Rev. D **65**, 013005 (2001); A. G. Dias, C. A. de S. Pires, and P. S. R. da Silva, Phys. Rev. D **68**, 115009 (2003); L. N. Hoang and D. V. Soa, Nucl. Phys. **B601**, 361 (2001); D. Ng, Phys. Rev. D **49**, 4805 (1994); J. T. Liu and D. Ng, Z. Phys. C **62**, 693 (1994).
[12] See for instance M. A. Pérez, G. Tavares-Velasco, and J. J. Toscano, Phys. Rev. D **69**, 115004 (2004).
[13] G. Aad *et al.* (ATLAS Collaboration), arXiv:0901.0512.
[14] R. Foot, O. F. Hernández, F. Pisano, and V. Pleitez, Phys. Rev. D **47**, 4158 (1993).
[15] D. Ng, Phys. Rev. D **49**, 4805 (1994); J. T. Liu and D. Ng, Z. Phys. C **62**, 693 (1994).
[16] A. G. Dias, R. Martínez, and V. Pleitez, Eur. Phys. J. C **39**, 101 (2005); A. G. Dias, Phys. Rev. D **71**, 015009 (2005); R. Martínez and F. Ochoa, Eur. Phys. J. C **51**, 701 (2007).
[17] V. Pleitez and M. D. Tonasse, Phys. Rev. D **48**, 2353 (1993).
[18] G. Passarino and M. J. G. Veltman, Nucl. Phys. **B160**, 151 (1979).
[19] A. Flores-Tlalpa, J. Montaño, F. Ramírez-Zavaleta, and J. J. Toscano (work in progress).
[20] R. Mertig, M. Bohm, and A. Denner, Comput. Phys. Commun. **64**, 345 (1991).
[21] K. Hagiwara, R. D. Peccei, D. Zeppenfeld, and K. Hikasa, Nucl. Phys. **B282**, 253 (1987).
[22] G. J. van Oldenborgh, Comput. Phys. Commun. **66**, 1 (1991).
[23] C. Amsler *et al.* (Particle Data Group), Phys. Lett. B **667**, 1 (2008).
[24] P. Das, P. Jain, and D. W. McKay, Phys. Rev. D **59**, 055011 (1999).
[25] A. T. Alan, A. Senol, and N. Karagoz, Phys. Lett. B **639**, 266 (2006).
[26] E. Ramirez-Barreto, Y. A. Coutinho, and J. Sá Borges, Eur. Phys. J. C **50**, 909 (2007).
[27] A. G. Dias, J. C. Montero, and V. Pleitez, Phys. Lett. B **637**, 85 (2006).
[28] D. L. Anderson and M. Sher, Phys. Rev. D **72**, 095014 (2005); A. C. Carcamo, R. Martínez, and F. Ochoa, Phys. Rev. D **73**, 035007 (2006).